

Linear Rayleigh-Taylor instability in an accelerated Newtonian fluid with finite width

S. A. Piriz and A. R. Piriz*

Instituto de Investigaciones Energéticas (INEI), E.T.S.I.I., and CYTEMA, Universidad de Castilla-La Mancha, 13071 Ciudad Real, Spain

N. A. Tahir

GSI Helmholtzzentrum für Schwerionenforschung Darmstadt, Planckstrasse 1, 64291 Darmstadt, Germany

(Received 4 January 2018; published 9 April 2018)

The linear theory of Rayleigh-Taylor instability is developed for the case of a viscous fluid layer accelerated by a semi-infinite viscous fluid, considering that the top interface is a free surface. Effects of the surface tensions at both interfaces are taken into account. When viscous effects dominate on surface tensions, an interplay of two mechanisms determines opposite behaviors of the instability growth rate with the thickness of the heavy layer for an Atwood number $A_T = 1$ and for sufficiently small values of A_T . In the former case, viscosity is a less effective stabilizing mechanism for the thinnest layers. However, the finite thickness of the heavy layer enhances its viscous effects that, in general, prevail on the viscous effects of the semi-infinite medium.

DOI: [10.1103/PhysRevE.97.043106](https://doi.org/10.1103/PhysRevE.97.043106)**I. INTRODUCTION**

The Rayleigh-Taylor instability (RTI), taking place at the interface between two fluids when a denser medium lays atop a lighter one in a gravitational field g , is present in an enormous variety of physical systems [1–8], ranging from the quotidian spilling of water from a jar when it is inverted, to astrophysical phenomena like the ignition of a supernova or the formation of the spectacular structures observed by the Hubble telescope in the supernova remnants of the Crab and Eagle nebula [9,10]. It is also behind many geophysical processes, such as in the coastal upwelling [11], in the subduction phenomenon occurring at the convergent boundaries of the tectonic plates [12], and in salt dome formations, as well as in the regularly spaced volcanism observed in continental rifting [13–17]. It also plays a role in ocean dynamics [18], in the bioconvection observed in cell cultures [19], and in many industrial processes. Besides, it is one of the crucial issues in the research on inertial confinement fusion [20–27], and in many experiments on high-energy density physics (HEDP) [28–42].

The most simple configuration of two superposed semi-infinite media has been widely studied in a huge variety of situations. However, much less effort has been dedicated to the RTI involving finite width media, probably because despite its relevance in most of the above-mentioned processes, the analysis becomes more difficult, especially when a lighter fluid with finite density and viscosity beneath the heavy layer is involved. The first study of the RTI in finite width fluids was already performed by G. I. Taylor [2] for the simplest case of a single layer of ideal fluid ($\rho_1 = 0$), so that the Atwood number $A_T = (\rho_2 - \rho_1)/(\rho_2 + \rho_1) = 1$, where fluids “1” and “2” are the lighter and the heavier fluids, respectively (Fig. 1). In such a case, he found that the growth rate γ is independent of the layer thickness h ($\gamma = \sqrt{kg}$, where k is the perturbation wave

number). An extension of the Taylor’s result to $A_T < 1$ was given by Goncharov *et al.* [43], showing that for a fluid slab of finite width h , the growth rate becomes smaller and is given by the following expression:

$$\gamma = \sqrt{\frac{(\rho_2 - \rho_1)kg}{\rho_2 + \rho_1 \coth kh}}. \quad (1)$$

Actually, such a result was already contained in the previous work by Mikaelian in which he considered the RTI of stratified ideal fluids with interfacial surface tensions [44]. More recently a somewhat similar work was performed for studying RTI in stratified media in presence of magnetic fields [45,46].

Previous studies of RTI in stratified viscous fluids were carried on by Harrison in the framework of the equivalent problem of the oscillation of superposed fluids [47]. However, the final results were limited to the case of very low viscosity of the heavy layer. RTI in stratified fluids was also considered by several authors. For instance, Ramberg studied the problem for a variety of boundary conditions, but the particular case of an accelerated layer with a top free surface was barely mentioned [13,14]. A similar problem was investigated by Lister and Kerr [15], and by Wilcock and Whitehead [17], for the particular case of a very low viscosity of the heavy fluid slab. Besides, the complementary asymptotic regime of small wave Reynolds number (high viscosity or very large perturbation wave number) was considered by Parhi and Nath [16].

The RTI in situations in which the medium composing the slab is an elastic solid was also considered, although in much less extent [48,50,51].

The three-layer system with viscosity and surface tensions was also analyzed by Mikaelian for the case in which the system is confined by rigid walls [52,53]. However, in most of the experiments on HEDP, as well as in many situations present in Nature, we have to deal with a denser fluid slab of finite thickness pushed and accelerated by a lighter fluid. So that no rigid walls are present, and the top surface of the

*roberto.piriz@uclm.es

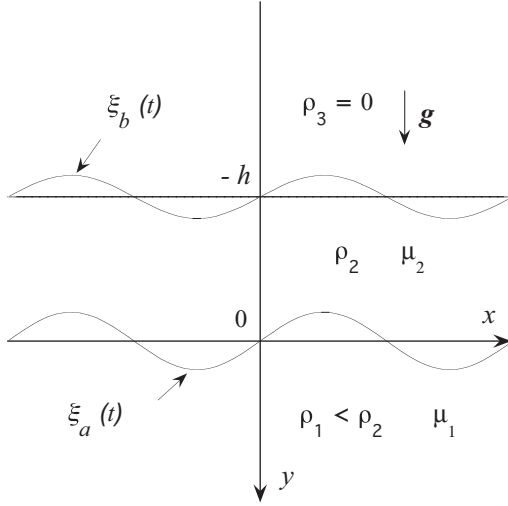


FIG. 1. Schematic of the two-interfaces system formed by a viscous layer on the top of a semi-infinite viscous fluid.

heavier medium is a free surface, such as in the case of the recent experiment by Adkins *et al.* [54].

Besides, a similar situation is expected to occur in the advanced target designs for inertial confinement fusion using ablaters of high density carbon or beryllium [55–57]. These ablaters are melted at the beginning of the target implosion for eliminating the deleterious effects of the polycrystalline microstructures present in the solid state which could seed hydrodynamic instabilities.

In this paper we study the RTI in a viscous fluid slab of width h , and density ρ_2 , laying atop a semi-infinite viscous fluid of lower density $\rho_1 < \rho_2$, with interfacial surface tension on each interface, and considering that the top interface is a free surface. To investigate the relative effects of the lighter fluid viscosity, and of the surface tensions, we first analyze the case in which the light fluid is ideal and with no surface tensions (Sec. II A). Later we include successively the effects of its viscosity, in an approximate manner by assuming that it is irrotational (Sec. II B), and the effects of the surface tensions on the interfaces (Sec. II C).

II. LINEAR ANALYSIS OF THE RTI

Figure 1 shows the general situation we are studying, consisting in a Newtonian fluid slab of width h , density ρ_2 , and dynamic viscosity μ_2 , overlaying a semi-infinite Newtonian fluid of density $\rho_1 < \rho_2$, and dynamic viscosity μ_1 , in a constant gravitational field $\vec{g} = g\hat{e}_y = -\vec{\nabla}\varphi$ (\hat{e}_y is the unitary vector in the vertical direction, and φ is the gravitational potential). The denser fluid occupies the region $-h \leq y \leq 0$, and the lighter fluid occupies the region $y \geq 0$. The region $y < -h$ above the fluid slab is empty ($\rho_3 = 0$).

We start with the equations for momentum and mass conservation, which read as follows:

$$\rho \frac{d\vec{v}}{dt} = -\vec{\nabla}p + \rho\vec{g} + \vec{\nabla} \cdot \vec{\sigma}', \quad (2)$$

$$\frac{d\rho}{dt} + \rho\vec{\nabla} \cdot \vec{v} = 0, \quad (3)$$

where \vec{v} , ρ , and p are the fluid velocity, density, and pressure, respectively. In addition, $\vec{\sigma}'$ is the deviatoric part of the stress tensor $\sigma_{ik} = -p\delta_{ik} + \sigma'_{ik}$ (δ_{ik} is the Kronecker δ), which for a Newtonian fluid is written in the following form

$$\sigma'_{ik} = \mu \left(\frac{\partial v_i}{\partial x_k} + \frac{\partial v_k}{\partial x_i} - \frac{2}{3}\delta_{ik} \frac{\partial v_j}{\partial x_j} \right), \quad (4)$$

where we have used index notation for Cartesian tensors in which any index $i, j, k = 1, 2, 3$ indicates the space coordinates x, y, z , respectively. Besides, in Eqs. (2) and (3), dM/dt represents the total material derivative of any magnitude M ($\vec{v}, \rho, p, \vec{\sigma}'$):

$$\frac{dM}{dt} = \frac{\partial M}{\partial t} + (\vec{v} \cdot \vec{\nabla})M. \quad (5)$$

For linearizing the previous equations we proceed in the usual manner by expressing every magnitude M as $M = M_0 + \delta M$, where M_0 and $\delta M \ll M_0$ are, respectively, the equilibrium value and the perturbation of M . Then, Eqs. (2)–(4) yield the following linear equations system for the perturbations:

$$\rho_n \frac{\partial(\delta\vec{v}_n)}{\partial t} = -\vec{\nabla}(\delta p_n + \rho_n \delta\varphi_n) + \vec{\nabla} \cdot \vec{S}^{(n)}, \quad (6)$$

$$\vec{\nabla} \cdot (\delta\vec{v}_n) = 0, \quad (7)$$

where $n = 1, 2$ refers to the bottom and top medium, respectively, and we have assumed incompressible perturbations ($\delta\rho = 0$). In addition, it is

$$S_{ik}^{(n)} \equiv \delta\sigma'_{ik} = \mu \left[\frac{\partial(\delta v_{ni})}{\partial x_k} + \frac{\partial(\delta v_{nk})}{\partial x_i} \right]. \quad (8)$$

To obtain the perturbed velocity field we use the Helmholtz decomposition [8, 58], for which we can express the velocity field as the sum of an irrotational part $\delta\vec{v}^\phi = \vec{\nabla}\phi$, determined by the scalar function ϕ , plus a rotational part $\delta\vec{v}^\psi$ given by the zero divergence vector $\psi\hat{e}_z$:

$$\delta\vec{v}_n = \vec{\nabla}\phi_n + \vec{\nabla} \times (\psi_n \hat{e}_z). \quad (9)$$

Then, substitution of Eq. (9) into Eqs. (6) and (7) yields, respectively:

$$\vec{\nabla} \left(\gamma\phi_n + \frac{\delta p_n}{\rho_n} + \delta\varphi_n \right) + \vec{\nabla} \times [(\gamma\psi_n - v_n \nabla^2 \psi_n)\hat{e}_z] = 0, \quad (10)$$

$$\nabla^2 \phi_n = 0, \quad (11)$$

where $v_n = \mu_n/\rho_n$ is the kinematic viscosity of fluid “ n ,” $\delta\varphi_n = -g\eta_n = -g\delta v_{ny}/\gamma$, and we have taken $\phi \propto \psi \propto e^{\gamma t}$, with γ being the instability growth rate.

Equation (10) can be decoupled by adopting the Bernoulli gauge [8], so that the terms between parenthesis are equal to zero separately:

$$\gamma\phi_n + \frac{\delta p_n}{\rho_n} + \delta\varphi_n = 0, \quad (12)$$

$$\gamma\psi_n = v_n \nabla^2 \psi_n. \quad (13)$$

Thus, by assuming two-dimensional perturbations of the form:

$$\phi_n \propto e^{qy} \sin kx, \quad (14)$$

$$\psi_n \propto e^{q_n y} \cos kx. \quad (15)$$

Equations (11) and (13) yield, respectively,

$$q = \pm k; \quad q'_n = \pm \lambda_n; \quad \lambda_n = \sqrt{k^2 + \frac{\gamma}{\nu_n}}. \quad (16)$$

Equations (14)–(16) allow for obtaining the velocity field in each fluid from Eq. (9).

A. Viscous layer atop a lighter ideal fluid

We analyze at a first place the simplest case in which the semi-infinite lighter fluid is inviscid ($\mu_1 = 0$) and the effects of surface tensions are not taken into account. Thus, the perturbed velocity field of the lighter fluid ($y \geq 0$) is obtained from Eqs. (9) and (11) ($\psi_1 = 0$):

$$\phi_1 = a_1 e^{-ky} e^{\gamma t} \sin kx, \quad \delta v_{1y} = \frac{\partial \phi_1}{\partial y}, \quad \delta v_{1x} = \frac{\partial \phi_1}{\partial x}, \quad (17)$$

where a_1 is a constant to be determined.

For the heavier viscous fluid in the region $-h \leq y \leq 0$ we can write the following convenient forms for the potential functions ϕ_2 and ψ_2 , respectively:

$$\phi_2 = \frac{a \cosh ky + b \cosh k(h+y)}{\sinh kh} e^{\gamma t} \sin kx, \quad (18)$$

$$\psi_2 = \frac{c \sinh \lambda y + d \sinh \lambda(h+y)}{\sinh \lambda h} e^{\gamma t} \cos kx, \quad (19)$$

where a , b , c , and d are constants to be determined together with a_1 and the growth rate γ from the boundary conditions at $y = 0$ and $y = -h$. Then, the velocity field is given by Eq. (9), which can be re-written as follows:

$$\delta v_{2y} = \frac{\partial \phi_2}{\partial y} - \frac{\partial \psi_2}{\partial x}, \quad \delta v_{2x} = \frac{\partial \phi_2}{\partial x} + \frac{\partial \psi_2}{\partial y}. \quad (20)$$

1. Boundary conditions at $y = 0$ and $y = -h$

The continuity of the tangential and normal stresses at $y = 0$ and $y = -h$, respectively, and the continuity of the normal velocity at $y = 0$ produce a close set of equations for determining the previous constants and the growth rate.

Since the region above the fluid slab is empty ($\rho_3 = 0$), and the bottom lighter fluid is ideal [$S_{xy}^{(1)}(y = 0) = 0$], the continuity of the tangential stresses on each interface read, respectively,

$$S_{xy}^{(2)}(y = 0) = 0; \quad S_{xy}^{(2)}(y = -h) = 0. \quad (21)$$

Then, from Eqs. (8) and (18)–(20), it is straightforward to get the following relationships:

$$d = -\frac{2k^2}{\lambda^2 + k^2} b; \quad c = -\frac{2k^2}{\lambda^2 + k^2} a. \quad (22)$$

In a similar manner, the continuity of the normal stresses $\delta \sigma_{yy}^{(n)} = -\delta p_n + S_{yy}^{(n)}$ at both interfaces are expressed as

follows:

$$-\delta p_2 + S_{yy}^{(2)} = -\delta p_1, \quad y = 0, \quad (23)$$

$$-\delta p_2 + S_{yy}^{(2)} = 0, \quad y = -h. \quad (24)$$

From Eq. (12) we have

$$-\delta p_2 = \gamma \rho_2 \phi_2 - \frac{\rho_2 g \delta v_{2y}}{\gamma}; \quad -\delta p_1 = \gamma \rho_1 \phi_1 - \frac{\rho_1 g \delta v_{1y}}{\gamma}. \quad (25)$$

Therefore, at $y = 0$, Eq. (23) yields

$$\gamma \phi_2 + 2\nu_2 \frac{\partial(\delta v_{2y})}{\partial y} - \frac{g \delta v_{2y}}{\gamma} = \frac{\rho_1}{\rho_2} \left(\gamma \phi_1 - \frac{g \delta v_{1y}}{\gamma} \right), \quad (26)$$

and at $y = -h$ Eq. (24) gives

$$\gamma \phi_2 + 2\nu_2 \frac{\partial(\delta v_{2y})}{\partial y} - \frac{g \delta v_{2y}}{\gamma} = 0. \quad (27)$$

On the other hand, the continuity of the normal velocity at $y = 0$ is expressed as follows:

$$\delta v_{2y}(0) = \delta v_{1y}(0), \quad (28)$$

which yields

$$a_1 = -(b + d). \quad (29)$$

2. Dispersion relation and instability growth rate

By using Eqs. (18)–(20), and introducing Eqs. (22) and (29) into Eq. (26), we get

$$aA + b \left[C - B + \frac{\rho_1}{\rho_2} \left(\frac{\gamma}{\nu_2} + \frac{kg}{\gamma \nu_2} \right) \right] = 0, \quad (30)$$

where A , B , and C are given by the following expressions:

$$A = \frac{(\lambda^2 + k^2)^2 \operatorname{csch} kh - 4k^3 \lambda \operatorname{csch} \lambda h}{\lambda^2 - k^2}, \quad (31)$$

$$B = kg / \gamma \nu_2, \quad (32)$$

$$C = \frac{(\lambda^2 + k^2)^2 \coth kh - 4k^3 \lambda \coth \lambda h}{\lambda^2 - k^2}. \quad (33)$$

In the same manner, from Eq. (27), we get

$$a(C + B) + bA = 0. \quad (34)$$

The system formed by Eqs. (30) and (34) allows for obtaining the instability growth rate by asking that its determinant be equal to zero:

$$C^2 - A^2 = B^2 - \frac{\rho_1}{\rho_2} (C + B) \left(B + \frac{\gamma}{\nu_2} \right). \quad (35)$$

Equation (35) is a rather complicated transcendental equation for the growth rate γ as a function of the perturbation wave number k , with the slab thickness h , the viscosity ν_2 of the heavier fluid, and densities ρ_2 and ρ_1 as parameters. To express it in a more explicit form it is convenient to introduce dimensionless magnitudes:

$$\kappa = \frac{k}{k_0}; \quad \sigma = \frac{\gamma}{\sqrt{k_0 g}}; \quad k_0 = \left(\frac{g}{\nu_2^2} \right)^{1/3}. \quad (36)$$

Then, after a tedious but straightforward algebra we get the following equation for the dimensionless growth rate σ as a function of the dimensionless wave number κ , with the parameters $A_T = (\rho_2 - \rho_1)/(\rho_2 + \rho_1)$ and $\alpha = k_0 h$:

$$\begin{aligned} & (2\kappa^2 + \sigma)^4 + 16\kappa^6(\kappa^2 + \sigma) - 8\kappa^3\sqrt{\kappa^2 + \sigma}(2\kappa^2 + \sigma)^2 \\ & \times [\coth \alpha\kappa \coth \alpha\sqrt{\kappa^2 + \sigma} - \operatorname{csch} \alpha\kappa \operatorname{csch} \alpha\sqrt{\kappa^2 + \sigma}] \\ & = M_{Ta}^2\sigma^2 - \left[\frac{1 - A_T}{1 + A_T}(\kappa + \sigma^2 + M_v) + M_{Tb} \right] \\ & \times [\kappa M_{Ta} + (2\kappa^2 + \sigma)^2 \coth \alpha\kappa \\ & - 4\kappa^3\sqrt{\kappa^2 + \sigma} \coth \alpha\sqrt{\kappa^2 + \sigma}], \end{aligned} \quad (37)$$

where M_{Ta} , M_{Tb} , and M_v are functions of κ related to the presence of the interfacial surface tensions and viscosity in the lighter fluid. For the present particular case, we have

$$M_{Ta} = 1; \quad M_{Tb} = 0; \quad M_v = 0. \quad (38)$$

A much simpler expression is obtained for the asymptotic regime $\kappa \rightarrow \infty$. Actually, an equation for the asymptotic growth rate σ_∞ is more conveniently obtained from Eqs. (31) and (32), which for $\kappa \gg 1$ read

$$A = \frac{2k^2(kh \cosh kh + \sinh kh)}{\sinh^2 kh}, \quad (39)$$

$$C = \frac{k^2(2kh + \sinh 2kh)}{\sinh^2 kh}. \quad (40)$$

Introducing these equations into Eq. (35), we get

$$4\kappa^2\sigma_\infty^2 + 2\frac{1 - A_T}{1 + A_T}\kappa\sigma_\infty - \frac{2A_T}{1 + A_T} = 0 \quad (41)$$

or

$$\sigma_\infty = \frac{1}{4\kappa} \left[\sqrt{\left(\frac{1 - A_T}{1 + A_T}\right)^2 + \frac{8A_T}{1 + A_T}} - \frac{1 - A_T}{1 + A_T} \right]. \quad (42)$$

As it can be seen, the asymptotic value σ_∞ of the dimensionless growth rate is independent of the thickness of the fluid slab, and it only depends on the Atwood number A_T . That is, the effects of the viscosity and of the finite thickness of the heavier fluid slab will be felt mainly at the small and intermediate values of the dimensionless perturbation wave number. Certainly, this is the foreseen behavior because for the largest values of the perturbation wave number the layer is seen as a semi-infinite medium.

In Fig. 2 we have represented the growth rate σ for several values of the dimensionless thickness $\alpha = k_0 h$ of the slab and Atwood numbers. Figure 2(a) shows that the maximum growth rate is higher for the thinnest slabs for the particular case of $A_T = 1$. This behavior may seem to be somewhat unexpected in view of the fact that for ideal fluids, Eq. (1) shows that the growth rate is smaller for the thinnest slabs, at least for the cases when a lighter fluid below is present ($A_T < 1$). When $\rho_1 = 0$, Eq. (1) shows that σ becomes independent of h .

Nevertheless, both features are consistent with each other and caused by the same physical event, such as it was shown in [50,51] for the case of an accelerated elastic solid slab. In fact, to completely appreciate such a fact, it is worth to remark first

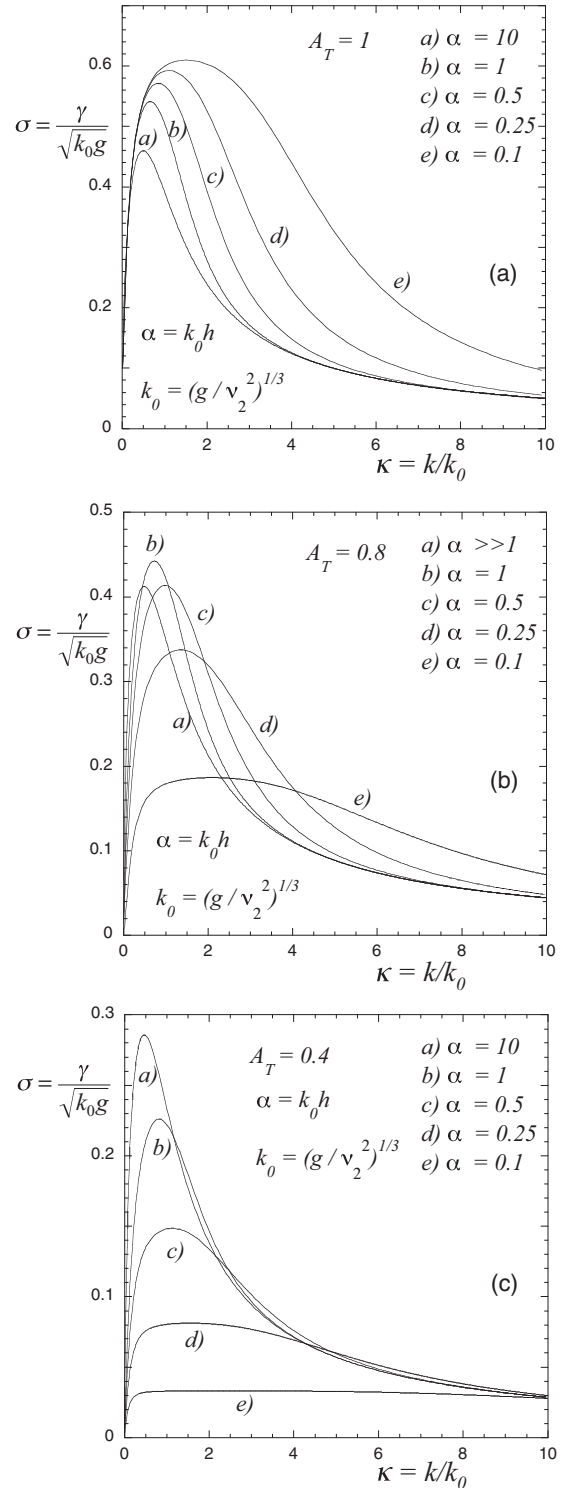


FIG. 2. Dimensionless growth rate σ as a function of the dimensionless perturbation wave number κ for several values of the dimensionless thickness $\alpha = k_0 h$ of the heavy fluid layer and different Atwood numbers A_T . (a) $A_T = 1$; (b) $A_T = 0.8$; (c) $A_T = 0.4$.

the physics underlying the growth rate reduction for thinner layers shown by Eq. (1) for ideal fluids.

From Fig. 1 we can see that as a consequence of the perturbation the weight per unitary surface increases in a

valley by the amount $\rho_2 g \Delta h$ ($\Delta h = \xi_a - \xi_b$), and if $\rho_1 = 0$ it drives the growth of the perturbation at the maximum rate [59]. Instead, when $\rho_1 \neq 0$, the lighter fluid exerts an opposite force (per unitary surface) $\rho_1 g \xi_a$ that slows down the instability growth. But since $\Delta h = \xi_a - \xi_b$ is greater as thicker is the slab whilst the force exerted by the lighter fluid is independent of h , the growth rate results to be larger for thicker slabs when two ideal fluids are involved.

If now $\rho_1 = 0$ ($A_T = 1$) and the slab consists of a viscous fluid, the force resisting the interface motion due to the viscosity is $S_{yy} \approx 2\mu_2\gamma(\Delta h/h)$. Since $\Delta h/h$ is larger for the thicker slabs, viscosity turns out more efficient for slowing down the instability growth. Then, the growth rate is smaller as thicker is the fluid slab, such as it is observed in Fig. 2(a).

When an ideal fluid beneath the viscous slab is present ($\rho_1 \neq 0$), the two previous effects arising from the thickness change Δh compete each other. This competition can be seen in Figs. 2(b) and 2(c). For $A_T = 0.8$, Fig. 2(b) shows that for the largest values of κ , the reduction of the effectiveness of the viscous forces lead to a higher growth rate for the thinnest slabs. But as κ decreases, the behavior inverts and the growth rates becomes smaller for the thinnest slabs as a consequence of the lower weight increase (in the valleys), together with the action of the buoyancy force $\rho_1 g \xi_a$ exerted by the lighter fluid. The second effect dominates for the thinnest slabs and $A_T = 0.8$, being the only effect that is operating for $A_T = 0.4$ at all the perturbation wave numbers and leading to the behavior shown in Fig. 2(c), in which the growth rate decreases for the thinner slabs. In any case, for the largest values of κ , the asymptotic regime is achieved and the dimensionless growth rate σ is determined only by the Atwood number [Eq. (42)].

On the other hand, the effect of the Atwood number alone is rather like expected, showing a reduction of the growth rate as lower is A_T , for a given value of α (Fig. 3).

B. Viscous layer atop a lighter viscous fluid

We include first the effect of the viscosity of the lighter fluid and we do this in an approximate manner by considering that the light fluid is irrotational [49,50]. As it was discussed in Ref. [50], this is a good approximation for $\kappa \ll 1$ and $\kappa \gg 1$, and the maximum error occurs for intermediate values of κ . However, it is well known that in the case of a single semi-infinite viscous fluid, the irrotational approximation produces pretty accurate results for the growth rate with a maximum error of around 11% when compared with the exact results [3]. In our case of two viscous fluids in which the irrotational approximation is used only in the semi-infinite lighter fluid, the goodness of the approximation can be expected to be better or, at most, equal than for the case of a single irrotational fluid.

Then, by adopting this approximation, the previous calculations presented in Sec. II A are modified by adding the following term on the right-hand side of Eq. (26):

$$\frac{\rho_1}{\rho_2} v_1 \frac{\partial(\delta v_{1y})}{\partial y}, \tag{43}$$

and the term M_v in Eq. (37) turns out

$$M_v = 2 \frac{v_1}{v_2} \kappa^2. \tag{44}$$

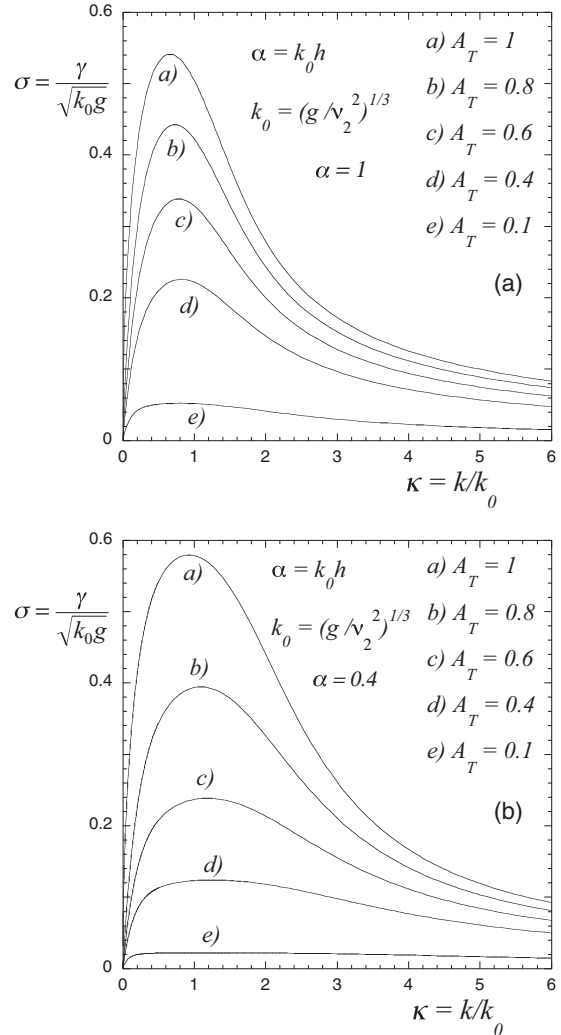


FIG. 3. Dimensionless growth rate σ as a function of the dimensionless perturbation wave number κ for several values of the Atwood number A_T and different dimensionless thicknesses $\alpha = k_0 h$. (a) $\alpha = 1$; (b) $\alpha = 0.4$.

As expected, in the case of two semi-infinite viscous fluids the accuracy of this approximation is better than for the case of a single viscous fluid, such as it can be seen in Fig. 4(a) where the results of the present theory for $\alpha \gg 1$ are compared with the exact calculations for several values of A_T [3]. We see that the accuracy is better than 5%.

In Fig. 4(b) we show the effect of the viscosity of the lighter fluid by comparing the case in which the lighter fluid is ideal with that one in which it has the same kinematic viscosity than the heavier fluid slab ($\nu_1 = \nu_2$). The effect of the light fluid viscosity is more pronounced for the largest values of the dimensionless perturbation wave number κ , where the growth rate reaches the asymptotic value and it becomes independent of α .

C. Viscous layer atop a lighter viscous fluid with surface tensions

To better appreciate the combined effects of viscosity and surface tension in a fluid slab accelerated by a semi-infinite

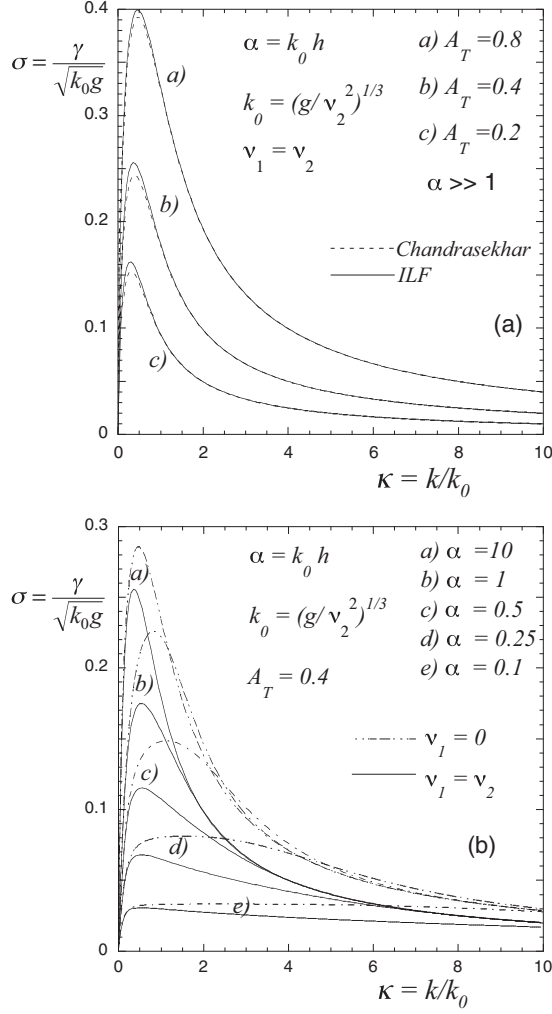


FIG. 4. Dimensionless growth rate σ as a function of the dimensionless perturbation wave number κ when both fluids are viscous ($v_1 = v_2$), and the lighter fluid is irrotational. (a) Comparison with exact rotational theory (Chandrasekhar) for the case of two semi-infinite fluids for several Atwood numbers A_T ; (b) Comparison with the case of an ideal light fluid ($v_1 = 0$) for several thicknesses $\alpha = k_0 h$ of the heavy layer.

fluid, let us first to briefly summarize the simpler case in which both fluid are inviscid and with surface tensions T_a and T_b at the interfaces $y = 0$, and $y = -h$, respectively. This case was already considered by Mikaelian for the more general situation including another ideal fluid above the layer ($\rho_3 \neq 0$) [44]. In the present case, the perturbation of the normal velocities can be written as follows:

$$\delta v_{2y} = (A_+ e^{ky} + A_- e^{-ky}) \sin kx; \quad -h \leq y \leq 0, \quad (45)$$

$$\delta v_{2y} = B_- e^{-ky} \sin kx; \quad -h \leq y \leq 0. \quad (46)$$

Then, the boundary conditions at $y = 0$ are

$$B_- = A_+ + A_- = \gamma \xi_a, \quad (47)$$

$$\frac{\gamma^2 \rho_1}{k} \xi_a + \frac{\gamma \rho_2}{k} (A_+ - A_-) = (\rho_2 - \rho_1) g \xi_a - k^2 T_a \xi_a, \quad (48)$$

and, at $y = -h$, we have

$$A_+ e^{-kh} + A_- e^{kh} = \gamma \xi_b, \quad (49)$$

$$\frac{\gamma \rho_2}{k} (A_+ e^{-kh} - A_- e^{kh}) = \rho_2 g \xi_b + k^2 T_b \xi_b. \quad (50)$$

By solving the system of Eqs. (47)–(50), the following bi-quadratic equation is obtained [44]:

$$c_1 \gamma^4 + c_2 \gamma^2 - c_3 = 0, \quad (51)$$

where

$$c_1 = \left(1 - \frac{\rho_1}{\rho_2}\right) \left(1 + \frac{\rho_1}{\rho_2} \coth kh\right), \quad (52)$$

$$c_2 = k^3 \left(\frac{T_b}{\rho_2} + \frac{T_a}{\rho_2 - \rho_1}\right) \coth kh + \frac{\rho_1}{\rho_2 - \rho_1} \left(kg + \frac{k^3 T_b}{\rho_2}\right) \left(1 + \frac{\rho_1}{\rho_2} \coth kh\right), \quad (53)$$

$$c_3 = \left(kg + \frac{k^3 T_b}{\rho_2}\right) \left(kg - \frac{k^3 T_a}{\rho_2 - \rho_1}\right). \quad (54)$$

Equations (51)–(54) show the well known fact that the surface tension T_a of the interface at $y = 0$ determines a cutoff wave number above which the system is stable, and that it is independent of the heavy layer width:

$$k_c = \sqrt{\frac{(\rho_2 - \rho_1)g}{T_a}}. \quad (55)$$

We will see that this value of k_c is not altered by the presence of the viscosities.

By simple inspection of Eqs. (48) and (50) we observe that surface tensions at both interfaces can be included in our more general problem by performing the following changes in Eqs. (26) and (27), at $y = 0$ and $y = -h$, respectively:

$$g \rightarrow g - \frac{k^2 T_a}{\rho_2 - \rho_1}; \quad y = 0, \quad (56)$$

$$g \rightarrow g + \frac{k^2 T_b}{\rho_2}; \quad y = -h. \quad (57)$$

With these transformations, in Eq. (37) for the instability growth rate, we have to take

$$M_{T_a} = 1 + S_a \kappa^2; \quad S_a = \sqrt{\frac{k_0}{g}} \frac{T_a}{\rho_2 v_2}, \quad (58)$$

$$M_{T_b} = \kappa^3 (S_a + S_b); \quad S_b = \sqrt{\frac{k_0}{g}} \frac{T_b}{\rho_2 v_2}. \quad (59)$$

In Figs. 5(a)–5(c) we have represented the growth rate as a function of the perturbation wave number for several values of the dimensionless fluid slab thickness α , and for different values of the Atwood number and of the dimensionless parameters S_a and S_b that determine the relative weight of the surface tension with respect to the viscous effects. The results are shown for a typical case with $v_1 = v_2$ (same kinematic viscosities). For comparison, we also show the corresponding growth rates for the case in which both fluids are inviscid, and for the case in which only the lighter fluid is inviscid.

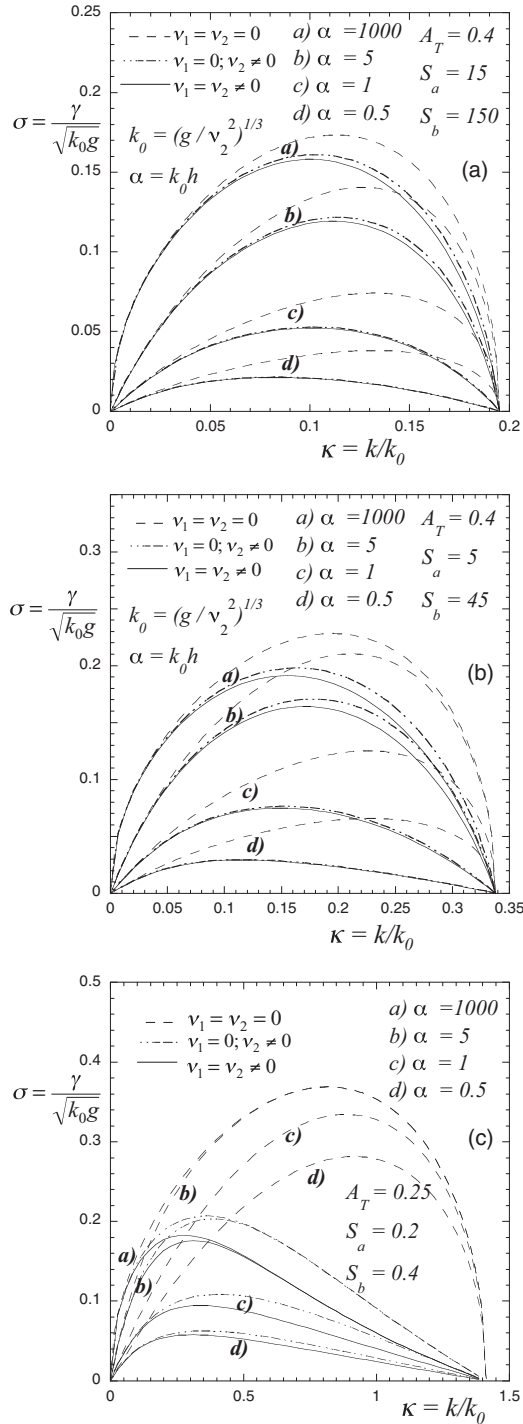


FIG. 5. Dimensionless growth rate σ as a function of the dimensionless perturbation wave number κ for several values of the dimensionless thickness $\alpha = k_0 h$ of the heavy fluid layer, and of the dimensionless surface tensions S_a and S_b . Comparisons with the cases of two ideal fluids ($v_1 = v_2 = 0$), and of a light ideal fluid ($v_1 = 0, v_2 \neq 0$). (a) $A_T = 0.4$, $S_a = 15$, $S_b = 150$; (b) $A_T = 0.4$, $S_a = 5$, $S_b = 45$; (c) $A_T = 0.25$, $S_a = 0.2$, $S_b = 0.4$.

As a general feature the viscosity of the lighter fluid beneath the viscous layer has, in relative terms, very little effect on the growth rate. This is essentially because the effects of the semi-infinite lighter fluid viscosity are more notorious for the

largest perturbation wave numbers, which are stabilized by the presence of the surface tension at the interface $y = 0$. This behavior is certainly more marked for the largest Atwood numbers for which the general role of the lighter fluid is diminished.

Therefore, the dominant viscous effects are, in general, linked to the viscosity of the heavier fluid layer. That is, the finite thickness of this layer enhance the effectiveness of the heavier fluid viscosity for reducing the instability growth rate. Such effects are, as in the previous cases, more significant for the largest perturbation wave numbers, close to the cutoff. On the other hand, as it could be expected, the role of viscosity is reduced for the largest values of S_a and S_b .

1. Comparison with experiments in Ref. [54]

The situation studied in this subsection has been recently considered experimentally by Adkins *et al.* [54]. They have performed very singular experiments with Newtonian fluids in a three layer system. One of these experiments corresponds to the case with $\rho_3 = 0$ that we are studying and, therefore, we can compare their experimental results with the present theory.

Actually, in the absence of a more complete theory as the presented in this work, the authors have compared their results with the inviscid theory by Mikaelian [44], which includes surface tension. However, they did not find a good quantitative agreement, and it was attributed to the viscosity of the involved fluids, not included in the Mikaelian's theory. In an attempt to present the results in a manner that hopefully could be independent of the fluid viscosities, they normalized the experimental results for the case of a finite thickness layer, with those ones corresponding to two semi-infinite fluids. These normalized experimental results were compared with the normalized theoretical results by using the Mikaelian's theory, and a good agreement was found, although no justification was given for such a procedure.

The present theory including viscosities and surface tensions does not provide any indication that the normalization procedure adopted in Ref. [54] could make the results independent of the fluid viscosities. Except, of course, for the trivial case in which viscosities are not relevant. In Figs. 6(a) and 6(b) we have represented the growth rate σ as a function of the perturbation wave number κ , for $A_T = 0.288$, $S_a = 15.91$, and $S_b = 141.4$, that correspond to the experimental conditions in Ref. [54] ($\rho_1 = 773 \text{ kg/cm}^3$, $\rho_2 = 1398 \text{ kg/cm}^3$, $T_a = 3.5 \times 10^{-3} \text{ N/m}$, $T_b = 31.1 \times 10^{-3} \text{ N/m}$, $\mu_1 = 3.26 \times 10^{-3} \text{ Pa s}$, $\mu_2 = 6.24 \times 10^{-3} \text{ Pa s}$), and for $\alpha = 7.897$, $\alpha = 15.794$, respectively, corresponding to the two fluid slab thicknesses used in the experiments ($h = 1 \text{ mm}$, and $h = 2 \text{ mm}$). The results for $\alpha \gg 1$ are also shown, as well as the corresponding cases for inviscid fluids (dotted lines). The experimental results are represented with full dots.

The two things to be noticed are that: (a) in agreement with the previous discussion, there are no significant differences between the inviscid theory and the present one including viscosities, for the relatively small perturbation wave numbers k considered in the experiments (1.257 mm^{-1} , 0.419 mm^{-1} , 0.314 mm^{-1} , 0.251 mm^{-1}); (b) as reported in Ref. [54] the theoretical values of the growth rate are larger than the ones observed in the experiments (around 20–25%). The first issue

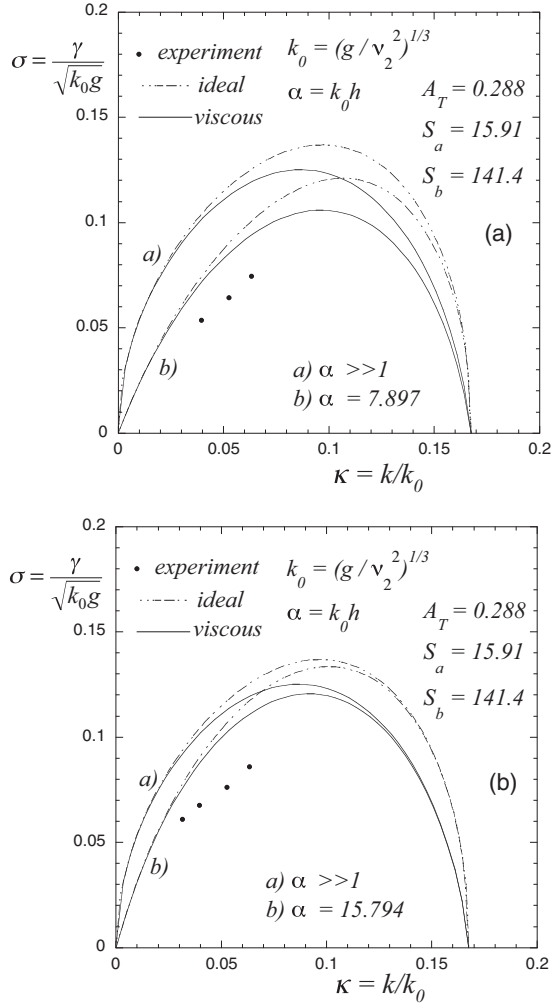


FIG. 6. Comparison of the present theory for two viscous fluids with surface tensions (full lines), with the experimental results (dots) of Ref. [54]. (a) $\alpha = 7.897$ ($h = 1$ mm); (b) $\alpha = 15.794$ ($h = 2$ mm). Results for the cases of two ideal fluids (dotted lines), and two semi-infinite fluids are also shown ($\alpha \gg 1$).

certainly explains that the normalization with the growth rates values for $\alpha \gg 1$ may agree with the experimental results, because in the range of perturbation wave numbers considered, viscosities have no significant effects.

However, the second issue cannot be explained. Perhaps, the fact that the normalized theoretical results agree with the experiments while the absolute values differ in more than a 20% in a range in which viscosity seems to play a not relevant role, may indicate the possibility of some systematic error in the measurements, the effects of which are canceled when the results are normalized with the corresponding growth rates for $\alpha \gg 1$.

III. CONCLUDING REMARKS

We have presented the linear theory of the incompressible RTI occurring when a semi-infinite viscous fluid pushes and accelerates a heavier viscous fluid layer of finite thickness h , including the effects of the surface tension on both interfaces and considering that the top interface is a free surface. This

is the situation of interest in most of the experiments on high energy density physics and, in particular, in the design of advanced targets for inertial confinement fusion that use high density carbon or beryllium as ablator materials. The internal microstructure due to the polycrystalline nature of such materials, together with the low density of the ablated corona does not allow to take advantage of their solid properties [51]. Therefore, the ablator must be melted by the first shock to avoid excessive seeding of the hydrodynamic instabilities [55–57].

It is found that when the effect of the surface tension is not dominant, there are two competing mechanisms that regulate the dependence of the instability growth rate in terms of the thickness of the heavy layer. Each one of such mechanisms prevail in an extreme value of the Atwood number. For $A_T = 1$ the growth rate is a decreasing function of the layer thickness, whilst the opposite is observed for $A_T \ll 1$. For intermediate values, the first behavior is ruling for large wave numbers κ and the second one for the smallest values of κ . This is because the viscosity becomes, in general, less effective for reducing the growth rate as thinner is the heavy layer. Therefore, the former behavior becomes weaker when the surface tension effects are dominant.

The viscosity of the semi-infinite lighter fluid is relatively less effective for reducing the growth rate than the viscosity of the heavier fluid layer, and since its effects are more notorious for the largest wave numbers κ , its influence becomes diminished when surface tension, which stabilizes such wave numbers, is present.

The theory can be applied to recent experiments reported in Ref. [54], and it shows that in the range of the experimental perturbation wave numbers, the growth rate is mainly determined by the surface tensions at both interfaces with a minor effect of the fluid viscosities. This certainly explains that the normalization of the experimental results with the corresponding growth rates for two semi-infinite fluids is in agreement with the normalized theoretical results by Mikaelian [44] for ideal fluids. But it could indicate that such a normalization procedure may have canceled eventual systematic errors in the experiment rather than the viscosity effects.

For applications to the design of advanced targets for inertial confinement fusion it would be necessary to know the mechanical properties of melted solids (surface tensions and viscosities) under the extremely high strain rates probably present during the target implosion. In this regards the present theory is also of relevance for the design of experiments using RTI as a tool for assessing such properties in a similar manner as it has been done for solid strength measurements at high strains and strain rates [35,36,39].

ACKNOWLEDGMENTS

This work has been partially supported by the Ministerio de Economía y Competitividad of Spain (Grant No. ENE2016-75703-R) and by the Bundesministerium für Bildung und Forschung (BMBF) of Germany. The authors are grateful to Prof. M. Bestehorn from Brandenburg University of Technology, Germany, for very interesting discussions.

- [1] Lord Rayleigh, *Scientific Papers*, Vol. II (Cambridge University Press, Cambridge, UK, 1900), pp. 200-207.
- [2] G. I. Taylor, *Proc. R. Soc. London A* **201**, 192 (1950).
- [3] S. Chandrasekhar, *Hydrodynamics and Hydromagnetic Stability* (Dover, New York, 1961), pp. 428480.
- [4] D. H. Sharp, *Physica (Amsterdam D)* **12**, 3 (1984).
- [5] H. J. Kull, *Phys. Rep.* **206**, 197 (1991).
- [6] N. A. Inogamov, *Astrophys. Space Phys.* **10**, 1 (1999).
- [7] A. R. Piriz, O. D. Cortazar, J. J. López Cela, and N. A. Tahir, *Am. J. Phys.* **74**, 1095 (2006).
- [8] R. Menikoff, R. C. Mjølness, D. H. Sharp, C. Zemach, and B. J. Doyle, *Phys. Fluids* **21**, 1674 (1978).
- [9] V. Bychkov and M. A. Liberman, *Astron. Astrophys.* **302**, 727 (1995).
- [10] X. Ribeyre, V. T. Tikhonchuk, and S. Bouquet, *Phys. Fluids* **16**, 4661 (2004).
- [11] A. Cui and R. L. Street, *Environ. Fluid Mech.* **4**, 197 (2004).
- [12] D. L. Turcotte and G. Schubert, *Geodynamics* (Cambridge University Press, New York, 2002).
- [13] H. Ramberg, *Phys. Earth Planet. Interiors* **1**, 427 (1968).
- [14] H. Ramberg, *Phys. Earth Planet. Interiors* **1**, 448 (1968).
- [15] J. R. Lister and R. C. Kerr, *J. Fluid Mech.* **202**, 577 (1989).
- [16] S. Parhi and G. Nath, *Int. J. Engng Sci.* **29**, 1439 (1991).
- [17] W. S. D. Wilcock and J. A. Whithead, *J. Geophys. Res.* **96**, 12193 (1991).
- [18] R. W. Schmitt, *Sci. Am.* **272**, 70 (1995).
- [19] M. S. Plesset and C. G. Whipple, *Phys. Fluids* **17**, 1 (1974).
- [20] S. Atzeni and J. Meyer-ter-Vehn, *The Physics of Inertial Fusion* (Oxford University Press, New York, 2004).
- [21] A. R. Piriz, *Phys. Fluids* **31**, 658 (1988).
- [22] J. G. Wouchuk and A. R. Piriz, *Phys. Plasmas* **2**, 493 (1995).
- [23] R. Betti, V. N. Goncharov, R. L. McCrory, and C. P. Verdon, *Phys. Plasmas* **2**, 3844 (1995).
- [24] V. N. Goncharov, R. Betti, R. L. McCrory, P. Sorotokin, and C. P. Verdon, *Phys. Plasmas* **3**, 1402 (1996).
- [25] A. R. Piriz, J. Sanz, and L. F. Ibañez, *Phys. Plasmas* **4**, 1117 (1997).
- [26] A. R. Piriz and R. F. Portugues, *Phys. Plasmas* **10**, 2449 (2003).
- [27] S. A. Piriz, A. R. Piriz, and N. A. Tahir, *Phys. Plasmas* **16**, 082706 (2009).
- [28] R. P. Drake, *High-Energy- Density Physics* (Springer, The Netherlands, 2006).
- [29] J. J. López Cela, A. R. Piriz, M. C. Serna Moreno, and N. A. Tahir, *Laser Part. Beams* **24**, 427 (2006).
- [30] N. A. Tahir, V. V. Kim, A. V. Matvechev, A. V. Ostriker, A. V. Shutov, I. V. Lomonosov, A. R. Piriz, J. J. López Cela, and D. H. H. Hoffmann, *Laser Part. Beams* **26**, 273 (2008).
- [31] N. A. Tahir, A. Shutov, I. V. Lomonosov, A. R. Piriz, G. Wouchuk, C. Deutsch, D. H. H. Hoffmann, and V. E. Fortov, *High Energy Density Phys.* **2**, 21 (2006).
- [32] N. A. Tahir, R. Schmidt, A. Shutov, I. V. Lomonosov, A. R. Piriz, D. H. H. Hoffmann, C. Deutsch, and V. E. Fortov, *Phys. Rev. E* **79**, 046410 (2009).
- [33] J. F. Barnes, P. J. Blewett, R. G. McQueen, K. A. Meyer, and D. Venable, *J. Appl. Phys.* **45**, 727 (1974).
- [34] S. M. Bakhraikh, O. B. Drennov, N. P. Kovalev, A. I. Lebedev, E. E. Meshkov, A. L. Mikhailov, N. V. Neumerzhitsky, P. N. Nizovtsev, V. A. Rayevsky, G. P. Simonov, V. P. Solov'yev, and I. G. Zhidov, Lawrence Livermore National Laboratory Report No. UCRL-CR-126710 (1997), <https://www.osti.gov/scitech/servlets/purl/515973>.
- [35] D. H. Kalantar, B. A. Remington, J. D. Colvin, K. O. Mikaelian, S. V. Weber, L. G. Wiley, J. S. Wark, A. Loveridge, A. M. Allen, A. A. Hauer, and M. A. Meyers, *Phys. Plasmas* **7**, 1999 (2000).
- [36] B. A. Remington, P. Allen, E. M. Bringa, J. Hawreliak, D. Ho, K. T. Lorenz, H. Lorenzana, J. M. McNaney, M. A. Meyers, S. W. Pollaine, K. Rosolankova, B. Sadik, M. S. Schneider, D. Swift, J. Wark, and B. Yaakobi, *Mater. Sci. Tech.* **22**, 474 (2006).
- [37] A. R. Piriz, J. J. López Cela, and N. A. Tahir, *J. Appl. Phys.* **105**, 116101 (2009).
- [38] A. R. Piriz, J. J. López Cela, and N. A. Tahir, *Phys. Rev. E* **80**, 046305 (2009).
- [39] H.-S. Park, K. T. Lorenz, R. M. Cavallo, S. M. Pollaine, S. T. Prisbrey, R. E. Rudd, R. C. Becker, J. V. Bernier, and B. A. Remington, *Phys. Rev. Lett.* **104**, 135504 (2010).
- [40] N. A. Tahir, P. Spiller, A. Shutov, I. V. Lomonosov, V. Gryaznov, A. R. Piriz, G. Wouchuk, C. Deutsch, F. Fortov, D. H. H. Hoffmann, and R. Schmidt, *Nucl. Instr. Meth. A* **577**, 238 (2007).
- [41] N. A. Tahir, I. V. Lomonosov, B. Borm, A. R. Piriz, A. Shutov, P. Neumayer, V. Bagnoud, and S. A. Piriz, *Ap. J. Suppl. Ser.* **232**, 1 (2017).
- [42] N. A. Tahir, V. Kim, A. Matvechev, A. Ostriker, A. V. Shutov, I. V. Lomonosov, A. R. Piriz, J. J. López Cela, and D. H. H. Hoffmann, *Nucl. Instrum. Methods B* **245**, 85 (2006).
- [43] V. N. Goncharov, P. McKenty, S. Skupsky, R. Betti, R. L. McCrory, and C. Cherfils-Clérouin, *Phys. Plasmas* **7**, 5118 (2000).
- [44] K. O. Mikaelian, *Phys. Rev. A* **26**, 2140 (1982).
- [45] Y. Y. Lau, J. C. Zier, I. M. Rittersdorf, M. R. Weis, and R. M. Gilgenbach, *Phys. Rev. E* **83**, 066405 (2011).
- [46] M. R. Weis, P. Zhang, Y. Y. Lau, I. M. Rittersdorf, J. C. Zier, R. M. Gilgenbach, M. H. Hess, and K. J. Peterson, *Phys. Plasmas* **21**, 122708 (2014).
- [47] W. Harrison, *Proc. Lond. Math. Soc.* **2**, 396 (1908).
- [48] B. J. Plohr and D. H. Sharp, *Z. Angew. Math. Phys.* **49**, 786 (1998).
- [49] D. Joseph, T. Funada, and J. Wang, *Potential Flows of Viscous and Viscoelastic Fluids* (Cambridge University Press, NY, 2007).
- [50] S. A. Piriz, A. R. Piriz, and N. A. Tahir, *Phys. Rev. E* **95**, 053108 (2017).
- [51] S. A. Piriz, A. R. Piriz, and N. A. Tahir, *Phys. Rev. E* **96**, 063115 (2017).
- [52] K. O. Mikaelian, *Phys. Rev. A* **42**, 7211 (1990).
- [53] K. O. Mikaelian, *Phys. Rev. E* **54**, 3676 (1996).
- [54] R. Adkins, E. M. Shelton, M.-Ch. Renoult, P. Carles, and C. Rosenblatt, *Phys. Rev. Fluids* **2**, 062001 (2017).
- [55] A. J. MacKinnon, N. B. Meezan, J. S. Ross, S. Le Pape, L. Berzak Hopkins, L. Divol, D. Ho, J. Milovich, A. Pak, J. Ralph, T. Doeppner, P. K. Patel, C. Thomas, R. Tommasini, S. Haan, A. G. MacPhee, J. McNaney, J. Caggiano, R. Hatarik, R. Bionta, T. Ma, B. Spears, J. R. Rygg, L. R. Benedetti, R. P. J. Town, D. K. Bradley, E. L. Dewald, D. Fittinghoff, O. S. Jones, H. R. Robey, J. D. Moody, S. Khan, D. A. Callahan, A. Hamza, J. Biener, P. M. Celliers, D. G. Braun, D. J. Erskine, S. T. Prisbrey, R. J. Wallace, B. Koziowski, R. Dylla-Spears, J. Sater, G. Collins, E. Storm, W. Hsing, O. Landen, J. L. Atherton, J. D. Lindl, M. J. Edwards, J. A. Frenje, M. Gatu-Johnson, C. K. Li,

- R. Petraso, H. Rinderknecht, M. Rosenberg, F. H. Se guin, A. Zylstra, J. P. Knauer, G. Grim, N. Guler, F. Merrill, R. Olson, G. A. Kyrala, J. D. Kilkenny, A. Nikroo, K. Moreno, D. E. Hoover, C. Wild, and E. Werner, [Phys. Plasmas](#) **21**, 056318 (2014).
- [56] S. Opie, E. Loomis, P. Peralta, T. Shimada, and R. P. Johnson, [Phys. Rev. Lett.](#) **118**, 195501 (2017).
- [57] P. F. Knapp, M. R. Martin, D. H. Dolan, K. Cochrane, D. Dalton, J.-P. Davis, C. A. Jennings, G. P. Loisel, D. H. Romero, I. C. Smith, E. P. Yu, M. R. Weis, T. R. Mattsson, R. D. McBride, K. Peterson, J. Schwarz, and D. B. Sinars, [Phys. Plasmas](#) **24**, 042708 (2017).
- [58] H. Lamb, *Hydrodynamics* (Dover Publications, Inc., NY, 1945).
- [59] E. Ott, [Phys. Rev. Lett.](#) **29**, 1429 (1972).